

## Coconut Tree Stress Detection as an Indicator of Red Palm Weevil (RPW) Attack Using Sentinel Data

**Faradina Marzukhi**

School of Civil Engineering, Universiti Sains Malaysia (Engineering Campus), 14300, Nibong Tebal, Pulau Pinang, Malaysia

**Md Azlin Md Said**

School of Civil Engineering, Universiti Sains Malaysia (Engineering Campus), 14300, Nibong Tebal, Pulau Pinang, Malaysia

**Amirul Audi Ahmad**

Department of Surveying Science and Geomatics, Universiti Teknologi MARA Perlis Branch, 02600, Arau, Perlis, Malaysia

### ABSTRACT

The red palm weevil (RPW) is one of the worst destructive pests of palms in the world. This study focuses for the first time on the coconut tree stress detection and discrimination among different stages of red palm weevil (RPW) stress-attacks using vegetation indices (VI) and the percentage of accuracy assessed. Different spectral indices were assessed using Sentinel 2A data of year 2018. Based on field identification, four classes of coconut tree were considered and evaluated using visual maps of VI: severe, moderate, early and healthy coconut trees. Results showed that the vegetation indices Normalized Differenced Vegetation Index (NDVI), Renormalized Difference Vegetation Index (RDVI), SQRT (IR/R), Difference Vegetation Index (DVI) and Green Vegetation Index (GVI) are sensitive to coconut trees caused by RPW attacks. They discriminated among the considered classes with more than 50% accurate from census data of field observation compared with remote sensing data of Sentinel 2A image. Nevertheless, they express the healthiness of tree stress between 0.308 – 0.673 range with 55% to 91% accurate. According to these results, it was concluded that remote sensing technique using Sentinel 2A data is a promising alternative for RPW detection based on VI.

### Article History

Received : 28 August 2019

Received in revised form : 20 July 2020

Accepted : 11 August 2020

Published Online : 31 August 2020

### Keywords:

coconut palm, tree stress, red palm weevil, vegetation indices, Sentinel 2A

### Corresponding Author Contact:

faradinamarzukhi.fm@gmail.com

DOI: 10.11113/ijbes.v7.n3.459

1. Introduction

Red Palm Weevil (RPW) (Olivier) (Coleopteran: Curculionidae) is a key pest of coconut *Cocos nucifera* L. originating from South and South East Asian Countries (Fiaboe et al., 2013). It can be found in Asia Pacific region such as India, China, Japan, Malaysia, Philippines, Vietnam, Thailand and Sri Lanka (Food and Agriculture Organization of the United (FAO) & International Center for Advanced Mediterranean Agronomic Studies (CIHEAM), 2017), that has significantly expanded its geographical and host range during the last three decades. In the Middle East, RPW is causing wide spread damage to date palm *Phoenix dactylifera* L., having both agricultural impacts on the palm production and environmental impacts. The rapid spread of RPW is due to many circumstances such as late detection of infested palms improper disposal of infested trees, improper assessment of the risks, few natural enemies of the pest, difficulties in managing the mass trapping and lack engagement with coconut farmers (CABI, 2017).

Since today, there is no effective techniques applied to detect the RPW infestation at the early stage because the infestation not clearly visible and only can be seen until it become severe or the coconut tree falls down. Likewise, nobody can confirm the conditions inside the coconut tree whether it is destroyed or not and with or without visible signals of damages from the outside. According to Dembilio and Jacas (2010), the morphological and biological characteristics of each one developmental instars are various among researches. (El-Shafie et al., 2013; Ju et al., 2011; Salama et al., 2009; Faghih, 1996; Kalshoven et al., 1981)

To date, according to Department of Agriculture (DOA) Malaysia, the lifecycle of RPW is 2-5 days for egg, 25-105 days for larva, 14-21 days for pupae and 60 – 105 days of adult which is stipulated in the Standard Operating Procedure (SOP) Malaysia (2017) on controlling the pest of RPW in Malaysia (DOA, 2017). It means that it took about 3.5 month of repeat cycle. Table 1 lists the different biological parameters, established by previous researches for each one of the developmental instars of *R. ferrugineus*.

**Table 1** The development period of *R. ferrugineus*. (Adapted from: Ávalos et al., 2014; Dembilio & Jacas, 2010)

| Development period (days) |          |         |           | Previous researches      |
|---------------------------|----------|---------|-----------|--------------------------|
| Egg                       | Larva    | Pupae   | Total     |                          |
| 3 - 5                     | 33 - 46  | 20 - 36 | -         | (El-Shafie et al., 2013) |
| 3 - 4                     | 30 - 67  | 23 - 36 | -         | (Ju et al., 2011)        |
| -                         | 69 - 128 | 16 - 29 | -         | (Salama, et al., 2009)   |
| 1 - 6                     | 41 - 78  | 15 - 27 | -         | (Faghih, 1996)           |
| -                         | 44 - 210 | -       | 105 - 210 | (Kalshoven et al., 1981) |

For instance, the extremity of the palm leafstalks become worn and histolytic with yellowish and brown colour, as well the top

crown colour becomes pale-green. The green leaves around the palm crown may deform due to deterioration of the support axes, resulting in an umbrella-like appearance. A viscous and sticky brown liquid substance oozes out from small holes in the trunk of the palm trees, with emergence holes for the adult RPW occurring in the crown or trunk. Finally, the fine pieces of chewed-up fibers emerge from the points (Bannari et al., 2016). In the previous researches, several methods have been implemented including which introduced by the Integrated Pest management (IPM). This include controlling and monitoring in ecology (e.g. insects and surroundings), biology (lifecycle), physical (pheromone trap) and chemical (e.g. pesticide and trunk injection). Apart from that, several advanced early detection methods also have been proposed including visual inspection (CABI, 2017), acoustic sensor (Victoria Soroker et al., 2016; Mankin, 2012; Siriwardena et al., 2010), thermal imaging (Golomb et al., 2015; V. Soroker et al., 2013), specially trained sniffer dogs (Nakash et al., 2000). All these have been tested and investigated in order to assist in identifying the infestation at the early stages. However, each of these methods has encounter many issues especially in implementation because of different problems occur with different conditions. Based on the literature review, the symptomatology of a palm tree infested by *R. ferrugineus* varies depending on the palm tree species, infestation level, and attack area. In order to identify those symptoms, especially on the early stage of infestation, the lifecycle (i.e. from egg to larva, pupae and adult instars) of the present and absent insects need to be confirmed. The coconut tree may show different stage of severity which similar to severity level of palm species as outlined by V. Soroker (2013) in Table 2.

**Table 2** The stage of Severity of RPW infestation at palm tree (V. Soroker et al., 2013)

| Stages of Severity |  |
|--------------------|--|
| Stage              | Description  |
| 1                  | Two differences – frond in V shape or in a zigzag position, holes in one or more leaves.     |
| 2                  | Some leaves collapsed, asymmetric inner leaf growth.   |
| 3                  | Crown partially collapsed, no new inner leaves.  |
| 4                  | All crown leaves collapsed into “umbrella” shape, tree cannot be recovered and chopped down. |

Remote sensing technique is becoming an alternative as it can assist in detecting the attacks by RPW using the satellite imagery. The early stress detection of the tree before visual damage symptoms are detectable through vegetation indices over few decades of numerous study. (Lichtenthaler et al., 1996). Therefore, it is believed that different stage of coconut tree stress-attack can be differentiated using the empirical data with relation to spectral bands. The multispectral data of Sentinel 2A. Sentinel 2A comes with multispectral instrument (MSI) sensor with blue (band 2), green (band 3), red (band 4) and near infrared (band 8) at 10-meter spatial resolution. (SUHET, 2013). Additionally, Sentinel 2A image can access the vegetation status (Das et al., 2019; Sonobe et al., 2018) same like other multispectral images not only because of available

bands but the vegetated area which can be sensor-detected is not much comparable with other high resolution satellite such as SPOT and Landsat (Taylor et al., 2011). Thus, the suitable VI's can be identified based on the spectral bands. Table 3 below shows the spectral bands that are used with different algorithm of VIs'. The algorithm used the green (G) band, red (R) band infrared (IR) and near infrared (NIR) band of the spectral reflectance.

**Table 3** The algorithm of vegetation indices based on spectral bands

| Algorithm (VI)                      | Previous Implementation (Author, year) |
|-------------------------------------|--|
| $NDVI = (NIR - R) / (NIR + R)$      | (Rouse et al., 1974)                   |
| $RDVI = (NIR - R) / \sqrt{NIR + R}$ | (Roujean & Breon, 1995)                |
| $SQRT (IR/R) = \sqrt{NIR/R}$        |  |
| $DVI = NIR - R$                     | (Richardson & Wiegand, 1977)           |
| $GVI = (NIR - G) / (NIR + G)$       | (Gitelson et al., 1996)                |

The use of spectral vegetation indices, calculated as a ratio or normalized difference from near-infrared (NIR, 750–1350 nm) and visible bands, has become one of the most common remote-sensing approach to retrieve biophysical variables over the past three decades (Colwell, 1974; Tucker 1979; Sellers 1985). Among all of the VI algorithm used, GVI and RDVI is the later used compared to DVI and NDVI. GVI is first implemented by Gitelson et al. (1996) that based on green and NIR spectral band (Panda, Ames, & Panigrahi, 2010) while Roujean and Breon (1995) introduced RDVI. NDVI is frequently used among reserchers in many studies, but in high vegetation cover, this index is saturated and also its relation with biophysical vegetation is not linear ((Haboudane et al., 2004; Vescovo & Gianelle, 2008; Jiang et al., 2008; Baret & Guyot, 1991; Gitelson, 2004). In contrast, the non-saturated index can be seen in low vegetation cover has been discussed by Barati et al. (2011). Although this has long been the traditional medium to highlight a particular property of vegetation, the introduction of further methods for detecting the coconut tree stress using these indices are currently under-used in the commercial, government, and scientific communities.

## 2. Materials and Methods

### 2.1 Description of Study Area

The study employs one coconut plantation of two-hectare coverage in Arau, Perlis with the total number of 395 coconut tree as shown in Figure 1. The geographic extent of the coconut tree plantation is found between latitudes of 6°27'35.84"N to 6°27'25.27"N and longitudes of 100°16'54.9"E to 100°16'54.8"E. The ground data sampling is done by gathering the ground data (census) which were collected at every coconut tree stands using a handheld Global Positioning System (GPS)

unit (GPSMAP®62sc, Garmin Ltd., KS). The coordinate systems of the 395 samples were registered using World Geodetic System (WGS) 84 coordinate system. Then, the 395 ground data (census) will be compared with the VI extracted from the Sentinel 2A. The 395 sampling points will distinguish the severity level of coconut tree stress (i.e. healthy, early, moderate and severe). Apart from that, ground observations for vertical and horizontal control are recorded using GPS technique. The UAV image is used for reference (image to image registration) in order to geometric corrected the multispectral Sentinel 2A image of 2018 which is provided by the European Space Agency (ESA). This image is used to extract the VI for NDVI, RDVI, SQRT (IR/R), DVI and GVI in order to determine the coconut tree stress.

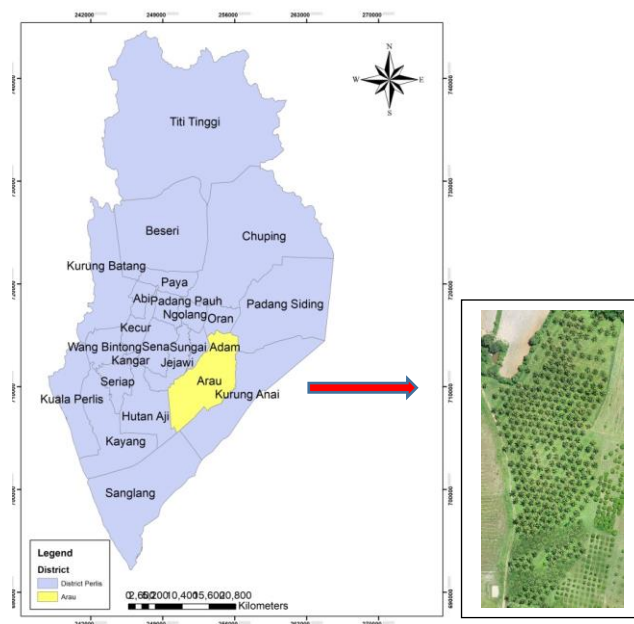


**Figure 1** Location of study area and ground data sampling

### 2.2 Image Processing and Accuracy Assessment

The raw data obtained from the satellite sensors has to undergo a few image pre-processing (Jensen & Lulla, 1987) such as image subset and image enhancement in order to maintain the quality of the satellite image. The image pre-processing and image processing is done by using ERDAS Imagine 2014 and ArcGIS 10.4 software. Next, the VI will be extracted, for example, the NDVI extracted values will be between -1 to +1 (Conte et al., 2007; Panda et al., 2010).

Supervised classification technique is used in this project for quantitative analysis of multispectral image data. The classification is done by clustering the pixels in a dataset into classes corresponding to the testing classes. There are many supervised classification techniques (Lillesand et al., 2004) including Mahalanobis, Minimum Distance, Parallelepiped, Maximum Likelihood and Spectral Angel Mapper (SAM). But in this project, Maximum Likelihood technique is implemented.

The actual (i.e. census) data and predicted (i.e. classified) is done by a classification system. The accuracies of the pixel based classifications obtained were evaluated in terms of overall accuracy, producer's accuracy, user's accuracy metrics (Congalton, 1991). The percentage of overall accuracy was calculated using the following formula:

$$\text{Overall accuracy} = \frac{\text{Total number of correct samples}}{\% \text{Total number of samples}} \times 100$$

### 3. Findings and Discussion

#### 3.1 Vegetation Indices

From our first visual analysis of the five VIs tested in this study, two provided results that showed some potential for correspondence with our field observations (Figure 2 and Figure 3). The NDVI enhanced the biomass density more than the GVI, which was expected because NDVI has been developed for purposes such as this. However, both indices show the top of the palm tree canopies almost uniformly with considerable biomass density. The spatial pattern discrimination of the various levels of attack is due to the palm tree crowns remaining green, despite earlier RPW attacks. Consequently, these VIs were sensitive only to vegetation cover and biomass density, but not to the pigmentation or physiological variation. Based on this visual analysis and interpretation, and the fieldwork (sampling and inspection), these VIs could discriminate among different levels of RPW stress- attack. This was confirmed by statistical regression tests that considered the four identified classes in the field (healthy; early attacked; moderate attacked; and severely attacked). For each class, 395 sampling points were located and the values of NDVI and GVI were extracted. Figure shows the results from first degree polynomial functions fitted through the full sample data set. For NDVI, the magnitude of separation amongst all classes was relatively high. NDVI showed a marginally better distinction between all classes however, it could significantly separate early and moderate attacked trees. Consequently, it is evident that the considered VIs extracted from Sentinel data are appropriate for RPW stress-attack detection.

It is clear from the results that, NDVI is the best reflectance index to explain variability of trees stress. The producer accuracy, user accuracy and overall accuracy are being accessed through four stages which are Healthy, Early, Moderate and Severe. The result of VI such as NDVI, RDVI, SQRT (IR/R), DVI and GVI are analyzed together with the severity level of coconut tree stress in a map representation (Figure 4 – 8). The map of coconut tree using the five methods are presented using green colour (lightness to brightness), orange and red colour to differentiate different stages of coconut tree stress. The method presented in this work is sufficiently general to be applied to classify the healthy and unhealthy coconut tree with respect to monitor vegetation characteristics (e.g. leaf area index (LAI), chlorophyll content, etc.)

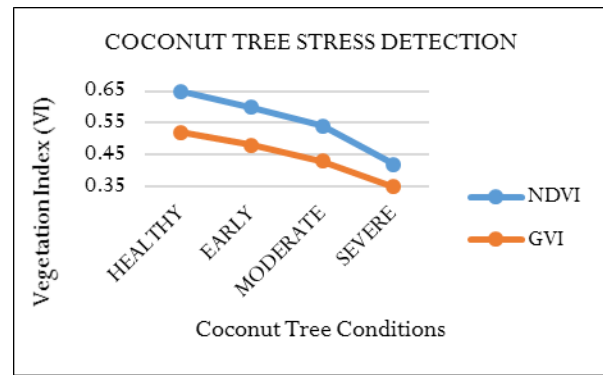


Figure 2 NDVI and GVI behavior for RPW stress-attack conditions

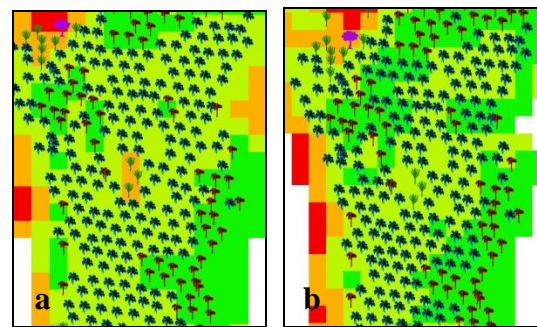


Figure 3 Derived maps of coconut trees: (a) NDVI; (b) GVI

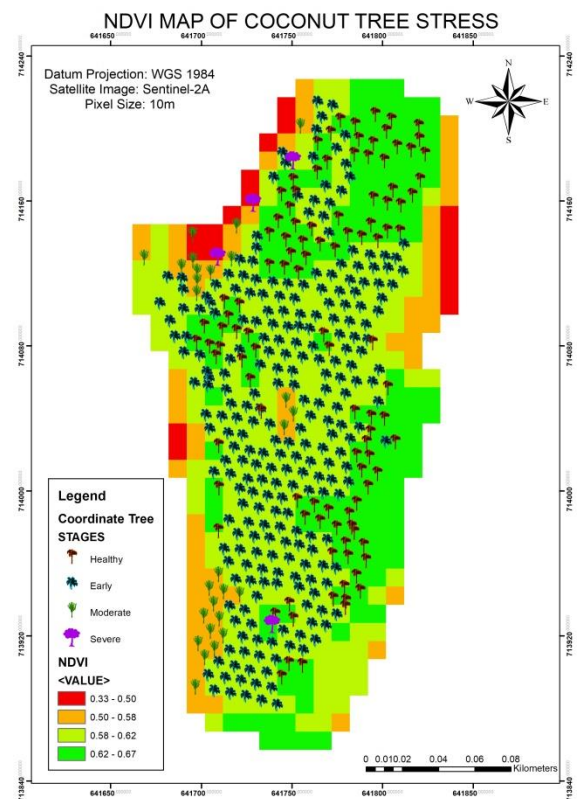


Figure 4 NDVI map of coconut tree stress

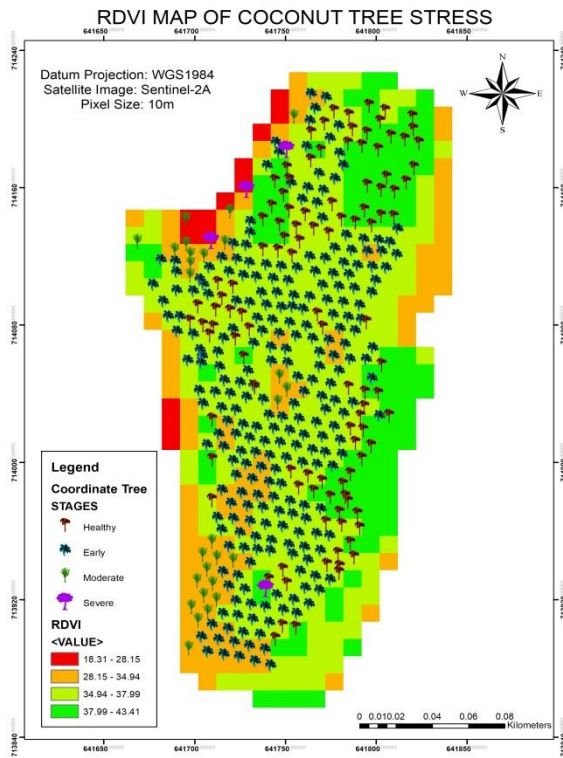


Figure 5 RDVI map of coconut tree stress

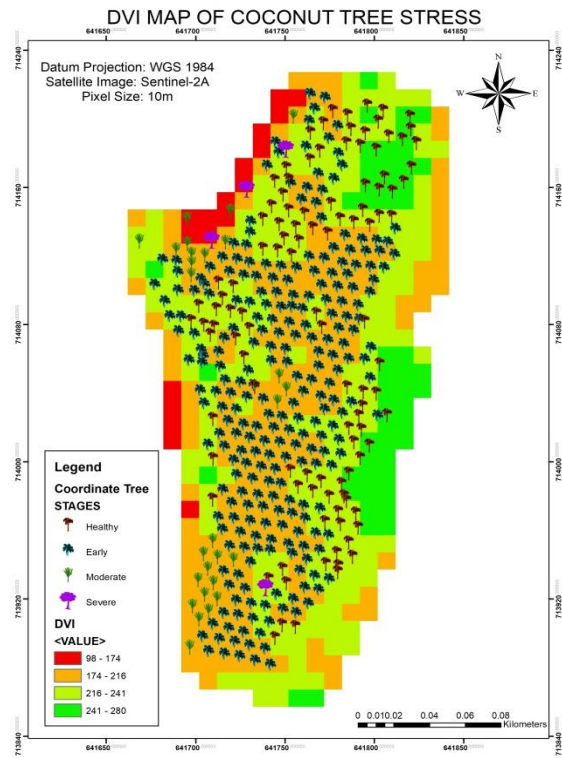


Figure 7 DVI map of coconut tree stress

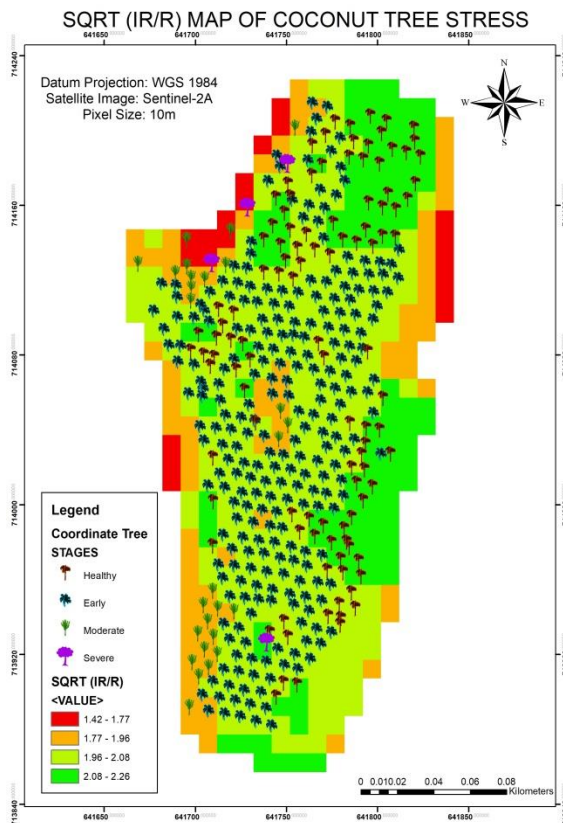


Figure 6 SQRT (IR/R) map of coconut tree stress

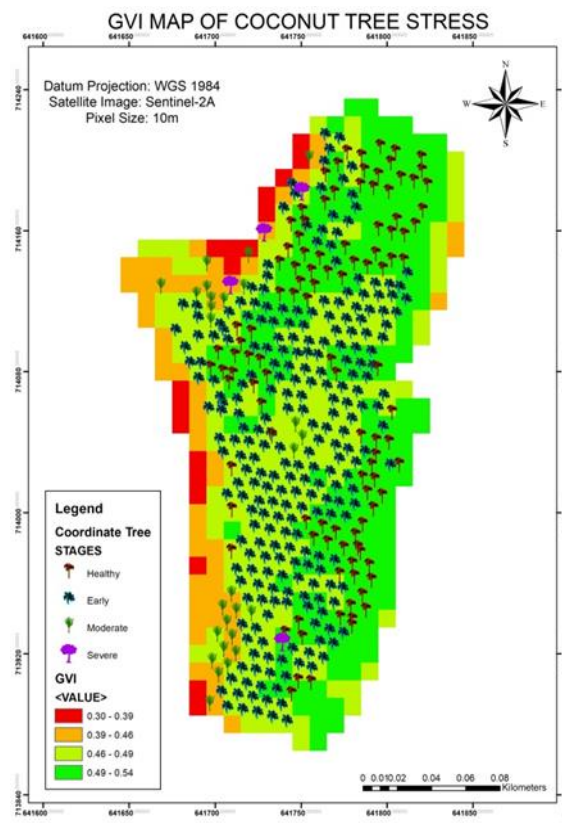


Figure 8 GVI map of coconut tree stress

The overall accuracy for NDVI, RDVI, SQRT (IR/R), DVI and GVI can be seen in Table 4 – 8 below. The highest accuracy is NDVI = 91% followed by SQRT (IR / R) = 71%, RDVI = 61%, GVI = 55% and the lowest accuracy is DVI = 30%.

**Table 4** Accuracy Assessment of NDVI method

|            |          | Actual  |       |          |        | Total |
|------------|----------|---------|-------|----------|--------|-------|
|            |          | Healthy | Early | Moderate | Severe |       |
| Classified | Healthy  | 97      | 2     | 0        | 1      | 100   |
|            | Early    | 12      | 236   | 0        | 0      | 248   |
|            | Moderate | 0       | 17    | 25       | 1      | 43    |
|            | Severe   | 0       | 0     | 2        | 2      | 4     |
|            | Total    | 109     | 255   | 27       | 4      | 395   |

|                  |     |
|------------------|-----|
| Overall Accuracy | 91% |
|------------------|-----|

**Table 5** Accuracy Assessment of SQRT (IR / R) method

|            |          | Actual  |       |          |        | Total |
|------------|----------|---------|-------|----------|--------|-------|
|            |          | Healthy | Early | Moderate | Severe |       |
| Classified | Healthy  | 59      | 1     | 0        | 1      | 61    |
|            | Early    | 49      | 193   | 0        | 0      | 242   |
|            | Moderate | 1       | 61    | 25       | 1      | 88    |
|            | Severe   | 0       | 0     | 2        | 2      | 4     |
|            | Total    | 109     | 255   | 27       | 4      | 395   |

|                  |     |
|------------------|-----|
| Overall Accuracy | 71% |
|------------------|-----|

**Table 6** Accuracy Assessment of RDVI method

|            |          | Actual  |       |          |        | Total |
|------------|----------|---------|-------|----------|--------|-------|
|            |          | Healthy | Early | Moderate | Severe |       |
| Classified | Healthy  | 28      | 0     | 0        | 0      | 28    |
|            | Early    | 81      | 185   | 1        | 2      | 269   |
|            | Moderate | 0       | 70    | 24       | 0      | 94    |
|            | Severe   | 0       | 0     | 2        | 2      | 4     |
|            | Total    | 109     | 255   | 27       | 4      | 395   |

|                  |     |
|------------------|-----|
| Overall Accuracy | 61% |
|------------------|-----|

**Table 7** Accuracy Assessment of GVI method

|            |          | Actual  |       |          |        | Total |
|------------|----------|---------|-------|----------|--------|-------|
|            |          | Healthy | Early | Moderate | Severe |       |
| Classified | Healthy  | 91      | 121   | 0        | 1      | 213   |
|            | Early    | 17      | 105   | 3        | 0      | 125   |
|            | Moderate | 1       | 28    | 21       | 1      | 51    |
|            | Severe   | 0       | 1     | 3        | 2      | 6     |
|            | Total    | 109     | 255   | 27       | 4      | 395   |

|                  |     |
|------------------|-----|
| Overall Accuracy | 55% |
|------------------|-----|

**Table 8** Accuracy Assessment of DVI method

|            |          | Actual  |       |          |        | Total |
|------------|----------|---------|-------|----------|--------|-------|
|            |          | Healthy | Early | Moderate | Severe |       |
| Classified | Healthy  | 12      | 0     | 0        | 0      | 12    |
|            | Early    | 93      | 82    | 1        | 2      | 178   |
|            | Moderate | 4       | 173   | 24       | 0      | 201   |
|            | Severe   | 0       | 0     | 2        | 2      | 4     |
|            | Total    | 109     | 255   | 27       | 4      | 395   |

|                  |     |
|------------------|-----|
| Overall Accuracy | 30% |
|------------------|-----|

**Table 9** The maximum and minimum index value of NDVI and GVI method

| Year (2018)   | NDVI  | GVI   |
|---------------|-------|-------|
| Maximum value | 0.673 | 0.548 |
| Minimum value | 0.339 | 0.308 |

Table 9 shows the contrast of maximum and minimum value of VI extracted from Sentinel-2A images in 2018. It can be concluded that NDVI and GVI give significant value of VI compared to DVI, RDVI and SQRT (IR/R). It shows that the healthiness of tree stress is ranged between 0.308 – 0.673.

**3.2 Comparison The Accuracies Of Different Vegetation Indices**

**Table 10** Correlation coefficient between vegetation indices for classified (from Sentinel data) and actual (from ground observation)

| Vegetation Index | NDVI   | GVI    | SQRT (IR/R) | RDVI   | DVI    |
|------------------|--------|--------|-------------|--------|--------|
| Correlation      | 0.996* | 0.567* | 0.917*      | 0.863* | 0.366* |

Note:\*\* Correlation is significant at the 0.05 level (two-tailed)

A Pearson correlation test showed that the relationship between classified vegetation index (i.e. NDVI) and actual vegetation index (Table 10) are statistically significant,  $r = 0.996$ ,  $p = .004$ .

**Table 11** Relationship between NDVI, GVI, SQRT (IR/R), RDVI and DVI indices and different curve estimation methods

| Method      | NDVI           |       | GVI            |       | SQRT (IR/R)    |       | RDVI           |       | DVI            |       |
|-------------|----------------|-------|----------------|-------|----------------|-------|----------------|-------|----------------|-------|
|             | R <sup>2</sup> | p     |
| Linear      | <b>0.993</b>   | 0.007 | 0.321          | 0.069 | 0.840          | 0.000 | 0.746          | 0.024 | 0.134          | 0.086 |
| Exponential | 0.789          | 0.021 | 0.643          | 0.038 | 0.660          | 0.034 | 0.508          | 0.049 | 0.172          | 0.082 |
| Logarithmic | 0.708          | 0.029 | 0.446          | 0.055 | 0.564          | 0.043 | 0.538          | 0.046 | 0.234          | 0.076 |
| Polynomial  | <b>0.993</b>   | 0.007 | 0.741          | 0.025 | 0.856          | 0.014 | 0.819          | 0.018 | <b>0.996</b>   | 0.004 |

Note: Bold values represent significant regressions with  $p < .05$

The polynomial method seems to be advantageous compared with the majority of studies on different vegetation indices (Table 11). In this analysis,  $R^2=0.558$  show that 55.8% of total variation in classified point of tree data is explained by the total variation of actual point of tree. However, the good fit model (refer Table 12; Model Summary, ANOVA and coefficients) is shown significant ( $p$ -value = .000). A regression parameter test showed that the relationship between actual point of tree and classified point of tree is statistical significant,  $p$ -value = .000. In details, for each additional actual point of tree, classified point of tree will significantly increase by 0.805 unit.

**Table 12** Analysis of regression parameter of classified and actual point of tree

| Model Summary                         |                   |                |                   |                            |      |      |
|---------------------------------------|-------------------|----------------|-------------------|----------------------------|------|------|
| Model                                 | R                 | R Square       | Adjusted R Square | Std. Error of the Estimate |      |      |
| 1                                     | .747 <sup>a</sup> | 0.558          | 0.533             | 68.891                     |      |      |
| a. Predictors: (Constant), classified |                   |                |                   |                            |      |      |
| ANOVA <sup>a</sup>                    |                   |                |                   |                            |      |      |
| Model                                 |                   | Sum of Squares | df                | Mean Square                | F    | Sig. |
| 1                                     | Regressi          | 1077           | 1                 | 107795.643                 | 22.7 | .000 |

|                                       | on         | 95.643                      |            |                           | 13    | <sup>b</sup> |
|---------------------------------------|------------|-----------------------------|------------|---------------------------|-------|--------------|
|                                       | Residual   | 85428.107                   | 18         | 4746.006                  |       |              |
|                                       | Total      | 193223.750                  | 19         |                           |       |              |
| a. Dependent Variable: actual         |            |                             |            |                           |       |              |
| b. Predictors: (Constant), classified |            |                             |            |                           |       |              |
| Coefficients <sup>a</sup>             |            |                             |            |                           |       |              |
| Model                                 |            | Unstandardized Coefficients |            | Standardized Coefficients | t     | Sig.         |
|                                       |            | B                           | Std. Error |                           |       |              |
| 1                                     | (Constant) | 19.235                      | 22.708     |                           | 0.847 | 0.408        |
|                                       | classified | 0.805                       | 0.169      | 0.747                     | 4.766 | 0.000        |
| a. Dependent Variable: actual         |            |                             |            |                           |       |              |

#### 4. Conclusion

The results indicate that VI such as NDVI and GVI as derived from Sentinel 2A multispectral imagery offer a potentially viable and important alternative for discrimination the severity level of RPW stress-attack. Therefore, it can be concluded from this positive results that this proposed method can be further testing with other open access data, perhaps analyze with other parameters that might influence the RPW outbreak especially on palm tree species.

#### Acknowledgements

The authors would like to thank the European Space Agency (ESA) for the remote sensing data given. They acknowledge the support of Mr. Mohd Ridzuan AB Jalil who is an assistant agriculture officer from Department of Agriculture (DOA), Malaysia for his field work assistance.

#### References

Ávalos, J. A., Martí-Campoy, A., & Soto, A. (2014). Study of the flying ability of *Rhynchophorus ferrugineus* (Coleoptera: Dryophthoridae) adults using a computer-monitored flight mill. *Bulletin of Entomological Research*, 104(4): 462–470.

Bannari, A., Mohamed, A. M. A., & Peddle, D. R. (2016). Biophysiological spectral indices retrieval and statistical analysis for red palm weevil stressattack prediction using Worldview-3 data. *International Geoscience and Remote Sensing Symposium (IGARSS)*, 3512–3515.

Barati, S., Rayegani, B., Saati, M., Sharifi, A., & Nasri, M. (2011). Comparison the accuracies of different spectral indices for estimation of

- vegetation cover fraction in sparse vegetated areas. *Egyptian Journal of Remote Sensing and Space Science*, 14(1): 49–56.
- Centre for Agriculture and Bioscience International CABI. (2017). "Red palm weevil datasheet. In: Invasive Species Compendium." Retrieved March, 10, 2017, from <http://www.cabi.org/isc/datasheet/47472>
- Colwell, J. E. (1974). Vegetation canopy reflectance. *Remote Sensing of Environment*, 3(3), 175–183.
- Congalton, R. G. (1991). A Review of Assessing the Accuracy of Classifications of Remotely Sensed Data, 46(October 1990), 35–46.
- Conte, A., Goffredo, M., Ippoliti, C., & Meiswinkel, R. (2007). Influence of biotic and abiotic factors on the distribution and abundance of *Culicoides imicola* and the *Obsoletus* Complex in Italy. *Veterinary Parasitology*, 150(4): 333–344.
- Das, B., Sahoo, R. N., Pargal, S., Krishna, G., Verma, R., Chinnusamy, V., ... Gupta, V. K. (2019). Comparative analysis of index and chemometric techniques-based assessment of leaf area index (LAI) in wheat through field spectroradiometer, Landsat-8, Sentinel-2 and Hyperion bands. *Geocarto International*, 0(0): 1–19.
- Dembilio, Ó., & Jacas, J. A. (2010). Basic bio-ecological parameters of the invasive Red Palm Weevil, *Rhynchophorus ferrugineus* (Coleoptera: Curculionidae), in phoenix canariensis under mediterranean climate. *Bulletin of Entomological Research*, 101(2): 153–163.
- DOA. (2017). *Prosedur Operasi Standard (SOP): Kawalan Perosak Kumbang Merah Palma (RPW)*. Jabatan Pertanian Malaysia.
- El-Shafie, H. A. ., Faleiro, J. R., & Aleid, S. M. (2013). *Full Length Research Paper A meridic diet for laboratory rearing of Red Palm Weevil , Rhynchophorus ferrugineus ( Coleoptera : Curculionidae )*, 8(39): 1924–1932.
- Faghieh, A. A. (1996). The biology of red palm weevil, *Rhynchophorus ferrugineus* Oliv. (Coleoptera, Curculionidae) in Saravan region (Sistan & Balouchistan province, Iran). *Applied Entomology and Phytopathology*, 63: 16-18.
- Fiaboe, K. K. M., Peterson, A. T., Kairo, M. T. K., & Roda, A. L. (2013). Predicting the Potential Worldwide Distribution of the Red Palm Weevil *Rhynchophorus ferrugineus* (Olivier) (Coleoptera: Curculionidae) using Ecological Niche Modeling . *Florida Entomologist*, 95(3): 659–673.
- Food and Agriculture Organization of the United (FAO) & International Center for Advanced Mediterranean Agronomic Studies (CIHEAM). (2017). "The Scientific Consultation and High-Level Meeting on Red Palm Weevil Management." Retrieved March, 13, 2017, from <http://www.fao.org/3/a-bu018e.pdf>
- Gitelson, A. A., Kaufman, Y. J., & Merzlyak, M. N. (1996). Use of a green channel in remote sensing of global vegetation from EOS-MODIS. *Remote Sensing of Environment*, 58(3): 289–298.
- Golomb, O., Alchanatis, V., Cohen, Y., Levin, N., Cohen, Y., & Soroker, V. (2015). Detection of red palm weevil infested trees using thermal imaging. *Precision Agriculture '15*: 643–650.
- Jensen, J. R., & Lulla, D. K. (1987). Introductory digital image processing: A remote sensing perspective. *Geocarto International*, 2(1): 65.
- Ju, R. T., Wang, F., Wan, F. H., & Li, B. (2011). Effect of host plants on development and reproduction of *Rhynchophorus ferrugineus* (Olivier) (Coleoptera: Curculionidae). *Journal of Pest Science*, 84(1): 33–39.
- Kalshoven, L. G. E., Laan, P. A. van der, & Rothschild, G. H. L. (1981). *Pests of crops in Indonesia*. Van Hoeve, Jakarta : P. T. Ichtiar Baru.
- Lichtenthaler, H. K., Lang, M., Sowinska, M., Heisel, F., & Miché, J. A. (1996). Detection of vegetation stress via a new high resolution fluorescence imaging system. *Journal of Plant Physiology*, 148(5): 599–612.
- Lillesand, T. M., Kiefer, R. W., & Chipman, J. W. (2004). *Remote Sensing and Image Interpretation* (5th ed.). Wiley.
- Mankin, R. W. (2012). Recent Developments in the use of Acoustic Sensors and Signal Processing Tools to Target Early Infestations of Red Palm Weevil in Agricultural Environments 1 . *Florida Entomologist*, 94(4): 761–765.
- Nakash, J., Osem, Y., & Kehat, M. (2000). A suggestion to use dogs for detecting red palm weevil (*Rhynchophorus ferrugineus*) infestation in date palms in Israel. *Phytoparasitica*, 28(2): 153–155.
- Panda, S. S., Ames, D. P., & Panigrahi, S. (2010). Application of vegetation indices for agricultural crop yield prediction using neural network techniques. *Remote Sensing*, 2(3): 673–696.
- Richardson, A. J., & Wiegand, C. L. (1977). Distinguishing vegetation from soil background information. *Photogrammetric Engineering and Remote Sensing*, 43(12): 1541–1552.
- Roujean, J., & Breon, F. (1995). Estimating PAR absorbed by vegetation from bidirectional reflectance measurements. *Remote Sensing of Environment*, 51(3): 375–384.
- Rouse, J. W., Hass, R. H., Schell, J. A., & Deering, D. W. (1974). Monitoring vegetation systems in the great plains with ERTS. *Third Earth Resources Technology Satellite (ERTS) Symposium*, 1: 309–317.
- Salama, H. S., Zaki, F. N., & Abdel-Razek, A. S. (2009). Ecological and biological studies on the red palm weevil *Rhynchophorus ferrugineus* (Olivier). *Archives of Phytopathology and Plant Protection*, 42(4): 392–399.
- Sellers, P. J. (1987). Canopy reflectance, photosynthesis, and transpiration, II. The role of biophysics in the linearity of their interdependence. *Remote Sensing of Environment*, 21(2), 143–183.
- Siriwardena, K. A. P., Fernando, L. C. P., Nanayakkara, N., Perera, K. F. G., Kumara, A. D. N. T., & Nanayakkara, T. (2010). Portable acoustic device for detection of coconut palms infested by *Rhynchophorus ferrugineus* (Coleoptera: Curculionidae). *Crop Protection*, 29(1): 25–29.
- Sonobe, R., Yamaya, Y., Tani, H., Wang, X., Kobayashi, N., & Mochizuki, K. (2018). Crop classification from Sentinel-2-derived vegetation indices using ensemble learning. *Journal of Applied Remote Sensing*, 12(02): 1.
- Soroker, V., A. La Pergula, Y. Cohen, V. Alchanatis, O Golomb., E. Goldshtein, M. Brandstetter. (2013). Early Detection and Monitoring

- of Red Palm Weevil: Approaches and Challenges. In *Association Française de Protection des Plantes (AFPP)- Palm Pest Mediterranean Conference Nice*.
- Soroker, V., Suma, P., La Pergola, A., Llopis, V. N., Vacas, S., Cohen, Y., Hetzroni, A. (2016). Surveillance Techniques and Detection Methods for *Rhynchophorus ferrugineus* and *Paysandisia archon*. *Handbook of Major Palm Pests: Biology and Management*, 209–232.
- SUHET. (2013). *SENTINEL-2 User Handbook*. European Space Agency.
- Taylor, S., Kumar, L., & Reid, N. (2011). Accuracy comparison of Quickbird, Landsat TM and SPOT 5 imagery for *Lantana camara* mapping. *Journal of Spatial Science*, 56(2): 241–252.
- Ávalos, J. A., Martí-Campoy, A., & Soto, A. (2014). Study of the flying ability of *Rhynchophorus ferrugineus* (Coleoptera: Dryophthoridae) adults using a computer-monitored flight mill. *Bulletin of Entomological Research*, 104(4), 462–470.
- Bannari, A., Mohamed, A. M. A., & Peddle, D. R. (2016). Biophysiological spectral indices retrieval and statistical analysis for red palm weevil stress attack prediction using Worldview-3 data. *International Geoscience and Remote Sensing Symposium (IGARSS)*, 3512–3515.
- Barati, S., Rayegani, B., Saati, M., Sharifi, A., & Nasri, M. (2011). Comparison the accuracies of different spectral indices for estimation of vegetation cover fraction in sparse vegetated areas. *Egyptian Journal of Remote Sensing and Space Science*, 14(1), 49–56.
- Centre for Agriculture and Bioscience International CABI. (2017). "Red palm weevil datasheet. In: *Invasive Species Compendium*." Retrieved March, 10, 2017, from <http://www.cabi.org/isc/datasheet/47472>
- Colwell, J. E. (1974). Vegetation canopy reflectance. *Remote Sensing of Environment*, 3(3), 175–183.
- Congalton, R. G. (1991). A Review of Assessing the Accuracy of Classifications of Remotely Sensed Data, 46(October 1990), 35–46.
- Conte, A., Goffredo, M., Ippoliti, C., & Meiswinkel, R. (2007). Influence of biotic and abiotic factors on the distribution and abundance of *Culicoides imicola* and the *Obsoletus* Complex in Italy. *Veterinary Parasitology*, 150(4), 333–344.
- Das, B., Sahoo, R. N., Pargal, S., Krishna, G., Verma, R., Chinnusamy, V., ... Gupta, V. K. (2019). Comparative analysis of index and chemometric techniques-based assessment of leaf area index (LAI) in wheat through field spectroradiometer, Landsat-8, Sentinel-2 and Hyperion bands. *Geocarto International*, 0(0), 1–19.
- Dembilio, Ó., & Jacas, J. A. (2010). Basic bio-ecological parameters of the invasive Red Palm Weevil, *Rhynchophorus ferrugineus* (Coleoptera: Curculionidae), in phoenix canariensis under mediterranean climate. *Bulletin of Entomological Research*, 101(2), 153–163.
- DOA. (2017). *Prosedur Operasi Standard (SOP): Kawalan Perosak Kumbang Merah Palma (RPW)*. Jabatan Pertanian Malaysia.
- El-Shafie, H. A., Faleiro, J. R., & Aleid, S. M. (2013). Full Length Research Paper A meridian diet for laboratory rearing of Red Palm Weevil, *Rhynchophorus ferrugineus* (Coleoptera: Curculionidae), 8(39), 1924–1932.
- Faghih, A. A. (1996). The biology of red palm weevil, *Rhynchophorus ferrugineus* Oliv. (Coleoptera, Curculionidae) in Saravan region (Sistan & Balouchistan province, Iran). *Applied Entomology and Phytopathology*, 63, 16–18.
- Fiaboe, K. K. M., Peterson, A. T., Kairo, M. T. K., & Roda, A. L. (2013). Predicting the Potential Worldwide Distribution of the Red Palm Weevil *Rhynchophorus ferrugineus* (Olivier) (Coleoptera: Curculionidae) using Ecological Niche Modeling. *Florida Entomologist*, 95(3), 659–673.
- Food and Agriculture Organization of the United (FAO) & International Center for Advanced Mediterranean Agronomic Studies (CIHEAM). (2017). "The Scientific Consultation and High-Level Meeting on Red Palm Weevil Management." Retrieved March, 13, 2017, from <http://www.fao.org/3/a-bu018e.pdf>
- Gitelson, A. A., Kaufman, Y. J., & Merzlyak, M. N. (1996). Use of a green channel in remote sensing of global vegetation from EOS-MODIS. *Remote Sensing of Environment*, 58(3), 289–298.
- Golomb, O., Alchanatis, V., Cohen, Y., Levin, N., Cohen, Y., & Soroker, V. (2015). Detection of red palm weevil infected trees using thermal imaging. *Precision Agriculture* '15, 643–650.
- Jensen, J. R., & Lulla, D. K. (1987). Introductory digital image processing: A remote sensing perspective. *Geocarto International*, 2(1), 65.
- Ju, R. T., Wang, F., Wan, F. H., & Li, B. (2011). Effect of host plants on development and reproduction of *Rhynchophorus ferrugineus* (Olivier) (Coleoptera: Curculionidae). *Journal of Pest Science*, 84(1), 33–39.
- Kalshoven, L. G. E., Laan, P. A. van der, & Rothschild, G. H. L. (1981). *Pests of crops in Indonesia*. Van Hoeve, Jakarta : P. T. Ichtiar Baru.
- Lichtenthaler, H. K., Lang, M., Sowinska, M., Heisel, F., & Miehé, J. A. (1996). Detection of vegetation stress via a new high resolution fluorescence imaging system. *Journal of Plant Physiology*, 148(5), 599–612.
- Lillesand, T. M., Kiefer, R. W., & Chipman, J. W. (2004). *Remote Sensing and Image Interpretation* (5th ed.). Wiley.
- Mankin, R. W. (2012). Recent Developments in the use of Acoustic Sensors and Signal Processing Tools to Target Early Infestations of Red Palm Weevil in Agricultural Environments 1. *Florida Entomologist*, 94(4), 761–765.
- Nakash, J., Osem, Y., & Kehat, M. (2000). A suggestion to use dogs for detecting red palm weevil (*Rhynchophorus ferrugineus*) infestation in date palms in Israel. *Phytoparasitica*, 28(2), 153–155.
- Panda, S. S., Ames, D. P., & Panigrahi, S. (2010). Application of vegetation indices for agricultural crop yield prediction using neural network techniques. *Remote Sensing*, 2(3), 673–696.
- Richardson, A. J., & Wiegand, C. L. (1977). Distinguishing vegetation from soil background information. *Photogrammetric Engineering and Remote Sensing*, 43(12), 1541–1552.
- Roujean, J., & Breon, F. (1995). Estimating PAR absorbed by vegetation from bidirectional reflectance measurements. *Remote Sensing of Environment*, 51(3), 375–384.

- Rouse, J. W., Hass, R. H., Schell, J. A., & Deering, D. W. (1974). Monitoring vegetation systems in the great plains with ERTS. *Third Earth Resources Technology Satellite (ERTS) Symposium*, 1, 309–317.
- Salama, H. S., Zaki, F. N., & Abdel-Razek, A. S. (2009). Ecological and biological studies on the red palm weevil *Rhynchophorus ferrugineus* (Olivier). *Archives of Phytopathology and Plant Protection*, 42(4), 392–399.
- Sellers, P. J. (1987). Canopy reflectance, photosynthesis, and transpiration, II. The role of biophysics in the linearity of their interdependence. *Remote Sensing of Environment*, 21(2), 143–183.
- Siriwardena, K. A. P., Fernando, L. C. P., Nanayakkara, N., Perera, K. F. G., Kumara, A. D. N. T., & Nanayakkara, T. (2010). Portable acoustic device for detection of coconut palms infested by *Rhynchophorus ferrugineus* (Coleoptera: Curculionidae). *Crop Protection*, 29(1), 25–29.
- Sonobe, R., Yamaya, Y., Tani, H., Wang, X., Kobayashi, N., & Mochizuki, K. (2018). Crop classification from Sentinel-2-derived vegetation indices using ensemble learning. *Journal of Applied Remote Sensing*, 12(02), 1.
- Soroker, V., A. La Pergola, Y. Cohen, V. Alchanatis, O Golomb., E. Goldshtein, M. Brandstetter. (2013). Early Detection and Monitoring of Red Palm Weevil: Approaches and Challenges. In Association Française de Protection des Plantes (AFPP)- Palm Pest Mediterranean Conference Nice.
- Soroker, V., Suma, P., La Pergola, A., Llopis, V. N., Vacas, S., Cohen, Y., Hetzroni, A. (2016). Surveillance Techniques and Detection Methods for *Rhynchophorus ferrugineus* and *Paysandisia archon*. *Handbook of Major Palm Pests: Biology and Management*, 209–232.
- SUIHET. (2013). SENTINEL-2 User Handbook. European Space Agency.
- Taylor, S., Kumar, L., & Reid, N. (2011). Accuracy comparison of Quickbird, Landsat TM and SPOT 5 imagery for Lantana camara mapping. *Journal of Spatial Science*, 56(2), 241–252.
- Tucker, C. J. (1979). Red and photographic infrared linear combinations for monitoring vegetation. *Remote Sensing of Environment*, 8(2), 127–150.